Journal of Superconductivity and Novel Magnetism (2020) 33:3015–3025
https://doi.org/10.1007/s10948-020-05591-2

ORIGINAL PAPER

Smart Metastructure Method for Increasing T_C of Bi(Pb)SrCaCuO High-Temperature Superconductors

Honggang Chen[1] · Yongbo Li[1] · Mingzhong Wang[1] · Guangyu Han[1] · Miao Shi[1] · Xiaopeng Zhao[1]

Received: 15 May 2020 / Accepted: 30 June 2020 / Published online: 5 July 2020

Abstract

Improving the critical transition temperature (T_C) of Bi(Pb)SrCaCuO (B(P)SCCO) high-temperature superconductors is important; however, considerable challenges exist. In this study, on the basis of the metamaterial structure and the idea that injecting energy will promote the formation of electron pairs, a smart meta-superconductor B(P)SCCO consisting of B(P)SCCO microparticles and Y_2O_3:Eu^{3+}+Ag or Y_2O_3:Eu^{3+} luminophore was designed. In the applied electric field, the Y_2O_3:Eu^{3+}+Ag or Y_2O_3:Eu^{3+} luminophore generates an electroluminescence (EL), thereby, promoting the T_C via EL energy injection. A series of Y_2O_3:Eu^{3+}+Ag or Y_2O_3:Eu^{3+} luminous inhomogeneous phase-doped B(P)SCCO samples was prepared. Meanwhile, the B(P)SCCO sample doped with 0.2 wt% Y_2O_3 or Y_2O_3:Sm^{3+} nonluminous inhomogeneous phase was also prepared. Results indicated that the T_C of 0.2 wt% Y_2O_3 or Y_2O_3:Sm^{3+} doping sample is lower than that of pure samples. However, the T_C of the sample doped with 0.2 wt% Y_2O_3:Eu^{3+}+Ag or Y_2O_3:Eu^{3+} luminophore is higher than that of pure sample. This outcome further demonstrated that the smart metastructure method can improve the T_C of B(P)SCCO.

Keywords Bi-based superconductors · Smart meta-superconductor B(P)SCCO · Y_2O_3:Eu^{3+}+Ag topological luminophore · Critical temperature · Energy injection

1 Introduction

Improving the critical transition temperature (T_C) of superconductors is important; however, considerable challenges exist. In 2011, Cavalleri et al. used a midinfrared femtosecond laser pulse to induce the transformation of $La_{1.675}Eu_{0.2}Sr_{0.125}CuO_4$ from a nonsuperconducting into a transient three-dimensional superconductor [1]. The behavior of transient superconducting transition in $La_{1.84}Sr_{0.16}CuO_4$, $YBa_2Cu_3O_{6.5}$, and K_3C_{60} was observed by using similar experimental methods [2–5]. The said researchers reported that laser pulse causes lattice distortion and induces transient superconductivity. Since then, the use of light to change the superconducting properties of materials has been gradually recognized. Scientists discovered the high-temperature superconductor BiSrCaCuO with a T_C beyond 100 K in 1988 [6, 7]. BiSrCaCuO superconductors are promising materials for theory research and industrial applications due to their several advantages, such as low oxygen sensitivity, containing no rare earth, and high T_C [6–9]. The BiSrCaCuO system consists of three superconducting phases with similar crystal structures, and its general formula can be written as $Bi_2Sr_2Ca_{n-1}Cu_nO_{2n+4}$, where $n = 1, 2$, and 3, with corresponding superconducting phases of Bi-2201 ($T_C = 20$ K), Bi-2212 ($T_C = 85$ K), and Bi-2223 ($T_C = 110$ K), respectively [10–17]. Pure Bi-2223 and Bi-2212 single phase are difficult to obtain because they are symbiotic with each other, especially when forming the Bi-2223 phase [18–21]. However, partial replacement of Bi by Pb can increase the volume content of the Bi-2223 phase, thereby, making it easy to synthesize and increasing its stability [22, 23].

Although Bi-based superconductors are called high-temperature superconductors, their critical parameters (especially the superconducting transition temperature T_C) are still far from the large-scale practical application. So Bi-based superconductors should be modified to increase their superconducting transition temperature T_C. At present, a commonly used method is chemical doping, for example, doping with elements, such as Cs [24], Al [25], Ce [26], and Pb [22, 23] in a Bi-Sr-Ca-Cu-O system. However, this method exhibits no significant increase in the superconducting transition

✉ Xiaopeng Zhao
xpzhao@nwpu.edu.cn

[1] Smart Materials Laboratory, Department of Applied Physics, Northwestern Polytechnical University, Xi'an 710129, China

temperature T_C. Subsequently, nanomaterials have been introduced for doping, for example, doping with Al_2O_3 [27], SnO_2 [28], ZrO_2 [29], MgO [30], $MgCO_3$ [31], and $Ca_2B_2O_5$ [32]. However, the results are unsatisfactory because most dopants are unstable at high temperature and react with the superconductor. Therefore, a suitable material for doping should be determined to ensure the stability at a high temperature and the increase of T_C.

Metamaterial, a type of artificially structured composite material, is composed of the matrix material and its unit material. The metamaterial properties are not primarily dependent on the matrix material but on the artificial structure. Many special functions can be obtained through various artificial structures [33–35]. With the development of metamaterial, the use of the metamaterial concept to design superconductors and affecting their T_C has been gradually recognized by scholars. In 2007, our group introduced inorganic electroluminescence (EL) material in superconductor to enhance the superconducting transition temperature through EL. Jiang et al. [36] first introduced uniformly distributed ZnO nano defects with a doping concentration of 1 wt% in Bi(Pb)SrCaCuO (B(P)SCCO) superconductors. The effects of different doping methods on the superconducting transition temperature and morphology of B(P)SCCO superconductors were investigated. The results of the standard four-probe method indicated that samples doped with ZnO EL material showed an evident performance belonging to high-temperature superconductor. However, the doping of ZnO EL materials caused a slight decrease of the B(P)SCCO superconducting transition temperature. Fundamentally, Y_2O_3:Eu^{3+} phosphor is an excellent rare earth luminescent material because of its several advantages, such as high luminescence intensity, good monochromaticity, and high quantum efficiency. And the preparation process of such material is simple, and the morphology is relatively easy to control. Moreover, the preparation of Y_2O_3:Eu^{3+} into a Y_2O_3:Eu^{3+}+Ag topological luminophore can further improve the EL properties of Y_2O_3:Eu^{3+} and have better stability in the environment [37–39]. Recently, Smolyaninov et al. [40–42] proposed that a superconducting metamaterial with an effective dielectric constant $\varepsilon_{eff} \approx 0$ may exhibit high transition temperature, and they confirmed their theory in experiment.

Our group recently selected traditional MgB_2 superconductor and constructed a smart meta-superconductor MgB_2 model based on the metamaterial structure. Smart meta-superconductor MgB_2 consists of the MgB_2 matrix and inhomogeneous phases, such as the EL material Y_2O_3:Eu^{3+} rods and different sizes of Y_2O_3:Eu^{3+} or YVO_4:Eu^{3+} sheets. The research results showed that the doping of EL materials increases the superconducting transition temperature of MgB_2. This increment is attributed to the EL materials that dispersed around MgB_2 particles. In the local electric field, the EL materials generate an EL. Therefore, the T_C of MgB_2 is improved by EL [43–47].

We select MgB_2 superconductor to construct a smart meta-superconductor MgB_2 based on the metamaterial structure and electron-phonon interaction in traditional MgB_2 superconductor. The electrons are transformed into Cooper pairs via energy injection by doping the Y_2O_3:Eu^{3+} EL material in MgB_2 superconductor, thereby, enhancing T_C of MgB_2 [45–47]. Many scientists believe that electron pairs are formed on the basis of the magnetic interaction of electron spin in the high-temperature superconductor B(P)SCCO [48, 49]. A smart meta-superconductor B(P)SCCO is proposed in this work, which consists of B(P)SCCO particles and Y_2O_3:Eu^{3+}+Ag or Y_2O_3:Eu^{3+} luminophore to form a composite particle structure. The B(P)SCCO superconducting particles are used as the matrix material, and the Y_2O_3:Eu^{3+}+Ag or Y_2O_3:Eu^{3+} luminophore inhomogeneous phase distributed around the B(P)SCCO particles. In the local electric field, the B(P)SCCO superconducting particles act as microelectrodes, which excite the EL of Y_2O_3:Eu^{3+}+Ag or Y_2O_3:Eu^{3+} luminophore, and EL energy injection will promote the formation of electron pairs, thus, changing the T_C of B(P)SCCO. The Y_2O_3:Eu^{3+}+Ag or $Y_2O_3Eu^{3+}$ luminophore–doped B(P)SCCO samples are prepared [50]. Results show that all samples have evident superconducting transition, and Y_2O_3:Eu^{3+}+Ag or $Y_2O_3Eu^{3+}$ luminophore–doped improves the superconducting transition temperature of B(P)SCCO superconductor. The nonluminous inhomogeneous phases Y_2O_3 and Y_2O_3:Sm^{3+} doping B(P)SCCO are prepared to further prove the effect of EL. The result shows that the nonluminous inhomogeneous phases Y_2O_3 and Y_2O_3:Sm^{3+} doping decreases the superconducting transition temperature.

2 Model

Figure 1 shows the microstructure model of the smart meta-superconductor B(P)SCCO based on the metamaterial structure. The black hexagons in this figure represent the B(P)SCCO superconducting particles, and the Y_2O_3:Eu^{3+}+

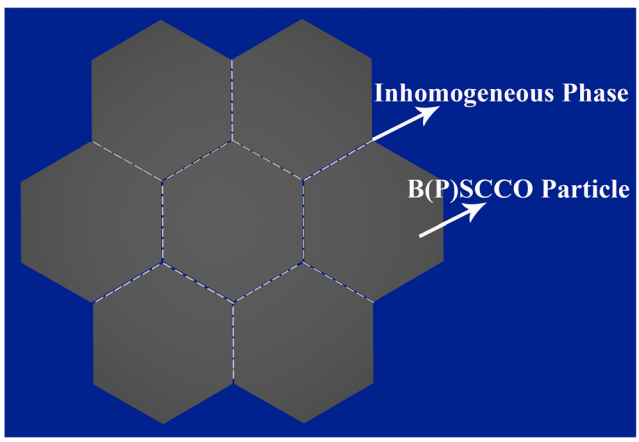

Fig. 1 The model of the smart metasuperconductor B(P)SCCO

Ag or Y_2O_3:Eu^{3+} luminophore inhomogeneous phase is dispersed around the B(P)SCCO particles, just like the discontinuous white ones in this figure. This model consists of B(P)SCCO superconducting particles and Y_2O_3:Eu^{3+}+Ag or Y_2O_3:Eu^{3+} luminophore to form a composite particle structure. The B(P)SCCO superconducting particles are used as the matrix material, and the Y_2O_3:Eu^{3+}+Ag or Y_2O_3:Eu^{3+} luminophore distributed around the B(P)SCCO particles are used as inhomogeneous phase dopants. When using a four-probe method in a liquid helium cryogenic system to measure the curve of the temperature dependence of resistivity (R–T) of the samples, the B(P)SCCO particles act as microelectrodes, which excite the EL of inhomogeneous phase EL materials, and EL energy injection will promote the formation of electron pairs. Thus the T_C of B(P)SCCO will be improved by EL energy injection. Adjusting the applied electric field to control the EL of Y_2O_3:Eu^{3+}+Ag or Y_2O_3:Eu^{3+} luminophore may alter the T_C of this smart meta-superconductor, thereby, achieving a smart meta-superconductor.

3 Experiment

3.1 Preparation of Inhomogeneous Phase Dopants

The preparation process of the topological luminophore Y_2O_3:Eu^{3+}+Ag (marked as N1) was described in detail in Ref. [37]. Y_2O_3 (marked as N2), Y_2O_3:Sm^{3+} (marked as N3) nonluminous inhomogeneous phases and Y_2O_3:Eu^{3+} (marked as N4) luminous inhomogeneous phase were obtained by changing the raw material.

3.2 Preparation of Pure B(P)SCCO Superconductor

A certain amount of raw material (all raw materials purity are 99% or 99.99%) was weighed according to the molar ratio of Bi_2O_3:PbO:$SrCO_3$:$CaCO_3$:CuO = 0.92:0.34:2.00:2.00:3.00. The powders were mixed and ground, followed by ball milling for 20 h at a speed of 500 r/min in an appropriate amount of anhydrous ethanol. The slurry was then dried at 60 °C to obtain gray powder. The dried gray powder was placed in a tube furnace, kept at 830 °C for 10 h, cooled to room temperature and then ground in an agate mortar. The process was repeated once to obtain B(P)SCCO calcined powder. The calcined powder was sufficiently ground and then kept at 10 MPa for 10 min to form a pellet of 12-mm diameter and 2-mm thickness. Finally, the pellet was placed in a tube furnace at 830 °C for 10 h to obtain a pure B(P)SCCO sample [50].

3.3 Preparation of Inhomogeneous Phase Doping B(P)SCCO Superconductors

Inhomogeneous phase dopants and B(P)SCCO calcined powder were mixed in 20 mL of ethanol and stirred 20 min with a magnetic stirrer to form a suspension. The suspension was transferred into a culture dish after 20 min of sonication and dried in a vacuum drying oven at 60 °C for 4 h to obtain black powder. The black powder was then fully ground and kept at 10 MPa for 10 min to form a pellet of 12-mm diameter and 2-mm thickness. Afterward, the pellet was placed in a tube furnace at 830 °C for 10 h to obtain the corresponding inhomogeneous phase doping B(P)SCCO sample [50]. We used two different purity raw materials to prepare nine types of doped samples, the contents, and types of dopants in all samples are shown in Table 1.

3.4 Characterization

X-ray diffraction patterns were obtained using an Hitachi XRD-7000 diffratometer with Cu Kα radiation in the range $3° \le 2\theta \le 60°$, at a scanning rate of 0.1°/s. A FEI Verios G4 scanning electron microscope (SEM) with an energy dispersion analysis X-ray (EDX) system was used to analyze the microstructural and phase formation, samples for the SEM studies were prepared by grinding sintered samples on SiC abrasive paper and performing gold spraying. The chemical composition of luminophore and doped samples were examined using photoelectron spectroscopy (XPS). The Axis Supra X-ray photoelectron spectroscopy was used to obtain the XPS signal intensity for individual elements. The determined binding energies were corrected to the energy of C 1 s peak at 284.5 eV, as reference BE position. CasaXPS software was used for XPS data processing.

Resistivity vs temperature measurements were performed on each of the sintered samples, approximately 12 mm in diameter and 2 mm in thickness, using the standard four-probe technique, in a liquid helium cryogenic system. 100, 10, 1, and 0.1 mA currents was applied. Keithley digital nanovoltmeter was used to measure the high resolution voltage across the sample. The voltage was determined by taking average value when the current was in the normal and reverse directions.

4 Results and Discussion

In order to prepare a metastructure superconductor consisting of B(P)SCCO superconductor and Y_2O_3:Eu^{3+}+Ag topological luminophore, we initially synthesized the Y_2O_3:Eu^{3+}+Ag topological luminophore. Figure 2a shows the EL spectrum of the Y_2O_3:Eu^{3+}+Ag topological luminophore. We also synthesized Y_2O_3:Sm^{3+} and Y_2O_3 dopants to further demonstrate the

Table 1 Purity, dopant and doping concentration of all the samples

Sample	A1	A2	A3	A4	A5	A6	B1	B2	B3	B4	B5
Purity (%)	99	99	99	99	99	99	99.99	99.99	99.99	99.99	99.99
Dopant	None	N1	N1	N1	N2	N3	None	N1	N4	N2	N3
Concentration (wt%)	0	0.1	0.2	0.5	0.2	0.2	0	0.2	0.2	0.2	0.2

effect of EL on metamaterial superconductor B(P)SCCO. Figure 2a also shows the EL spectrum of Y_2O_3:Eu^{3+}, Y_2O_3:Sm^{3+}, and Y_2O_3. The spectrum shows that a strong peak centered at 613 nm, which corresponds to Eu^{3+} ions typical of the transition from $^5D_0$ to $^7F_2$. The Y_2O_3:Eu^{3+} system formed by the nonluminous Y_2O_3 and luminous center Eu^{3+} ions is a strong luminophore. The EL intensity of Y_2O_3:Eu^{3+} can be further enhanced by Ag doping, and the EL intensity of the Y_2O_3:Eu^{3+}+Ag topological luminophore is considerably stronger than those of Y_2O_3:Sm^{3+} and Y_2O_3. Figure 2b shows the X-ray diffraction (XRD) pattern of the Y_2O_3:Eu^{3+}+Ag topological luminophore. The image indicates that the prepared Y_2O_3:Eu^{3+}+Ag topological luminophore is pure Y_2O_3, and no other impurity phases are detected. The Eu and Ag are added in small amounts; thus, no evident diffraction peak is found in the XRD pattern. Figure 2c–e show the scanning electron microscopy (SEM) and atomic force microscopy (AFM) images of the Y_2O_3:Eu^{3+}+Ag topological

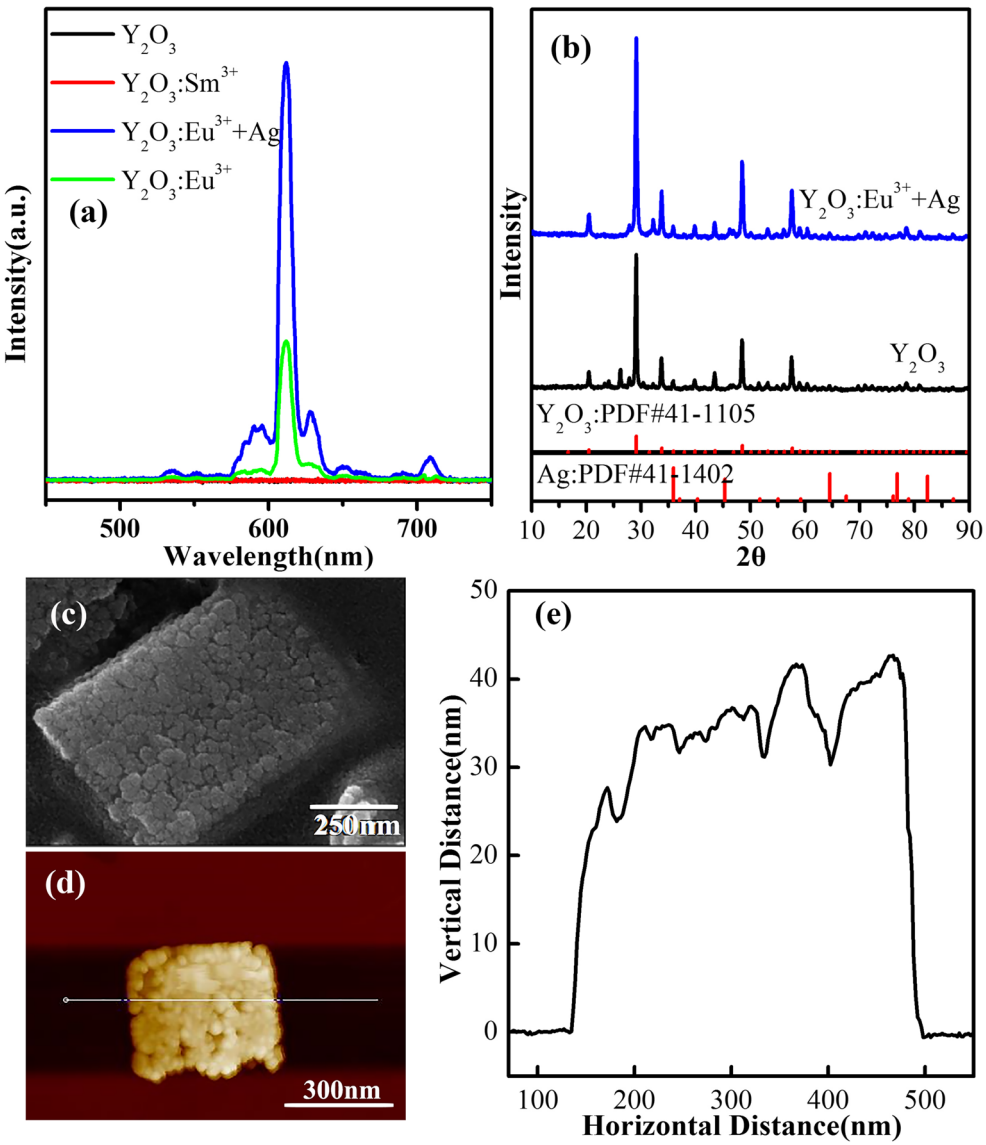

Fig. 2 **a** EL spectrum of Y_2O_3, Y_2O_3:Sm^{3+}, Y_2O_3:Eu^{3+}, and Y_2O_3:Eu^{3+}+Ag; **b** XRD, **c** SEM, and **d** AFM images of Y_2O_3:Eu^{3+}+Ag topological luminophore; **e** Height profile corresponding to the line draw in **d**

luminophore. The prepared Y_2O_3:Eu^{3+}+Ag topological luminophore dopant is a flake structure with a size of 300 × 400 nm, and a thickness of approximately 35 nm.

Figure 3 shows the XRD patterns of the pure B(P)SCCO sample (A1) and different inhomogeneous phase doping samples (A2, A3, A4, A5, and A6) prepared by solid-state sintering. The characteristic peaks of high-temperature phase Bi-2223 and low-temperature phase Bi-2212 are labeled by a rhombus and triangle, respectively. The peak positions and intensities of diffraction indicate that all samples comprise a mixture of high-temperature phase Bi-2223 and low-temperature phase Bi-2212, and no other impurity phases are detected. Besides, the addition of dopants has not introduced other impurity phases.

In this study, all peaks of the Bi-2223 and Bi-2212 phase have been used for the calculation of the volume content of the phases. The volume contents of the high-temperature phase Bi-2223 and low-temperature phase Bi-2212 calculated using the following equations [51, 52] are listed in Table 2:

$$\mathrm{Bi2223}(\%) \approx \frac{\sum I(Bi2223)}{\sum I(Bi2223) + \sum I(Bi2212)} \times 100\%,$$

$$\mathrm{Bi2212}(\%) \approx \frac{\sum I(Bi2212)}{\sum I(Bi2223) + \sum I(Bi2212)} \times 100\%,$$

where I is the intensity of the Bi-2223 and Bi-2212 phase in the XRD pattern (Fig. 3). Table 2 illustrates that the low-temperature phase Bi-2212 has a relatively large volume content in all prepared samples, and the volume contents of the high-temperature phase Bi-2223 in the doped samples are slightly decreased.

Figure 4a–d show the SEM images of the pure B(P)SCCO sample (A1), 0.2 wt% Y_2O_3:Eu^{3+}+Ag doped B(P)SCCO sample (A3), 0.2 wt% Y_2O_3 doped sample (A5), and 0.2 wt% Y_2O_3:Sm^{3+} doped sample (A6), respectively. The images

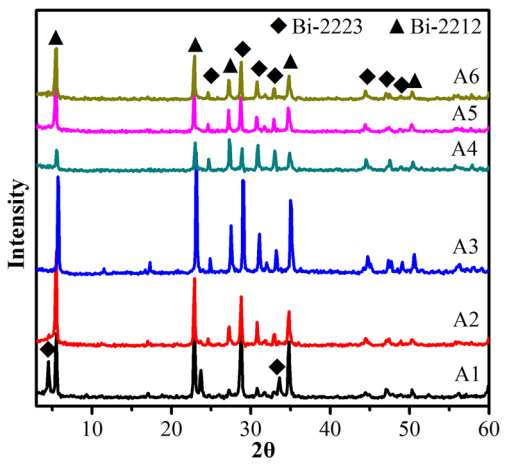

Fig. 3 X-ray diffraction patterns of pure B(P)SCCO (A1) and B(P)SCCO doped with 0.1 wt% Y_2O_3:Eu^{3+}+Ag (A2), 0.2 wt% Y_2O_3:Eu^{3+}+Ag (A3), 0.5 wt% Y_2O_3:Eu^{3+}+Ag (A4), 0.2 wt% Y_2O_3 (A5), and 0.2 wt% Y_2O_3:Sm^{3+} (A6)

Table 2 Summary of the volume content and critical temperature of A1, A2, A3, A4, A5, and A6

Sample	Bi-2223 (%)	Bi-2212 (%)	I = 100 mA	
			$T_{C,0}$ (K)	$T_{C,on}$ (K)
A1	46.8	53.2	57	101
A2	46.2	53.8	70	105
A3	45.1	54.9	65	105
A4	43.4	56.6	64	103
A5	44.8	55.2	58	98
A6	44.5	55.5	58	97

manifest that all the prepared samples are irregular block structure with a particle size of less than 2 μm. The addition of the dopants does not affect the microstructure of B(P)SCCO. Since the content of the Y_2O_3:Eu^{3+}+Ag topological luminophore in the doped sample is small, no flake inhomogeneous phase dopants are found in the doped samples, and no Y_2O_3 peaks are detected in the XRD pattern of the doped samples, so an elemental analysis and X-ray photoelectron spectrometric were performed. Figure 5 illustrates the distribution of certain chemical elements. The top left corner of each figure shows the corresponding element. Y was observed in the distribution of chemical elements, indicating the presence of the compound Y_2O_3 in the 0.5 wt% Y_2O_3:Eu^{3+}+Ag doped sample, and Y_2O_3 distributed around the B(P)SCCO particles. There were no obvious distribution of Eu and Ag due to their low content. In order to further confirm the presence of Eu and Ag, the XPS was performed. Figure 6a, b show the XPS spectra of Y_2O_3:Eu^{3+}+Ag topological luminophore and the 0.5 wt% Y_2O_3:Eu^{3+}+Ag doped B(P)SCCO sample (A4), respectively. The peaks of Eu 3d and Ag 3d were observed in the XPS spectra of Y_2O_3:Eu^{3+}+Ag topological luminophore (Fig. 6a), indicating that Eu and Ag were present in the topological luminophore. And Y was observed in SEM/EDS (Fig. 5) and the XPS (Fig. 6b) spectra of topological luminophore doped sample. Therefore, Y_2O_3:Eu^{3+}+Ag topological luminophore existed in the doped sample, and Y_2O_3:Eu^{3+}+Ag topological luminophore distributed around the B(P)SCCO particles.

Figure 7a presents temperature dependence of normalized resistivity (R–T) of the pure B(P)SCCO (A1), and B(P)SCCO doped with 0.1 wt% Y_2O_3:Eu^{3+}+Ag (A2), 0.2 wt% Y_2O_3:Eu^{3+}+Ag (A3), 0.5 wt% Y_2O_3:Eu^{3+}+Ag (A4), 0.2 wt% Y_2O_3 (A5), and 0.2 wt% Y_2O_3:Sm^{3+} (A6) with a test current of 100 mA. Figure 7b shows the $T_{C,0}$ and $T_{C,on}$ with error bars for A1, A2, A3, A4, A5, and A6. The electrical resistance is measured using the standard four-probe method. All prepared samples show a superconducting transition between 50 and 120 K. The two characteristic temperatures, namely, onset transition temperature $T_{C,on}$ and zero–

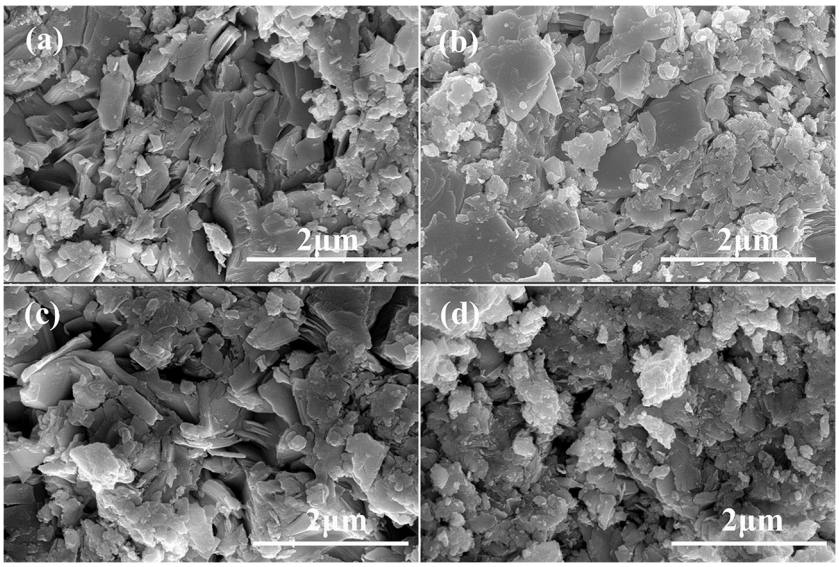

Fig. 4 SEM images of pure B(P)SCCO (A1) (**a**), and B(P)SCCO doped with 0.2 wt% Y_2O_3:Eu^{3+}+Ag (A3) (**b**), 0.2 wt% Y_2O_3 (A5) (**c**), and 0.2 wt% Y_2O_3:Sm^{3+} (A6) (**d**)

resistivity transition temperature $T_{C,0}$, on each *R–T* curve are discussed. $T_{C,on}$ and $T_{C,0}$ are defined by generally accepted standards in literatures [22, 53]. The resistivity temperature (*R–T*) curve exhibits metallic-like behavior between $T_{C,on}$ and room temperature. $T_{C,on}$ is the temperature at which the *R–T* curve deviates from linear behavior during cooling process, and the slope of the *R–T* curve changes significantly before and after this point. $T_{C,0}$ is the temperature at which the resistance just completely drops to zero. The black curve shows the *R–T* curve of pure B(P)SCCO. The $T_{C,0}$ and $T_{C,on}$ of pure B(P)SCCO are 57 K and 101 K, respectively. The low transition temperature may be due to the high testing current, low raw material purity, low sintering temperature, extremely short sintering time, and insufficient grinding of each sintering. The transition temperatures $T_{C,0}$ and $T_{C,on}$ of the Y_2O_3:Eu^{3+}+Ag topological luminophore doping samples exhibit an increase compared with the pure B(P)SCCO sample, which may be due to the Y_2O_3:Eu^{3+}+Ag topological luminophore distributed around B(P)SCCO particles to form a metamaterial structure with a special response, when testing the *R–T* curve of the sample, the B(P)SCCO particles act as microelectrodes, and the inhomogeneous phase EL materials would generate an EL; thereby, the T_C of B(P)SCCO can be improved by EL energy injection. The transition temperatures are listed in Table 2.

In order to further confirm whether the increase in transition temperature is the effect of EL or rare earth, the samples doped with 0.2 wt% Y_2O_3 and Y_2O_3:Sm^{3+} were prepared. It can be seen that the $T_{C,0}$ and $T_{C,on}$ of the 0.2 wt% Y_2O_3:Eu^{3+}+Ag topological luminophore doped sample show an obvious increase compared with the pure B(P)SCCO sample, and those of B(P)SCCO doped with 0.2 wt% Y_2O_3:Eu^{3+}+Ag

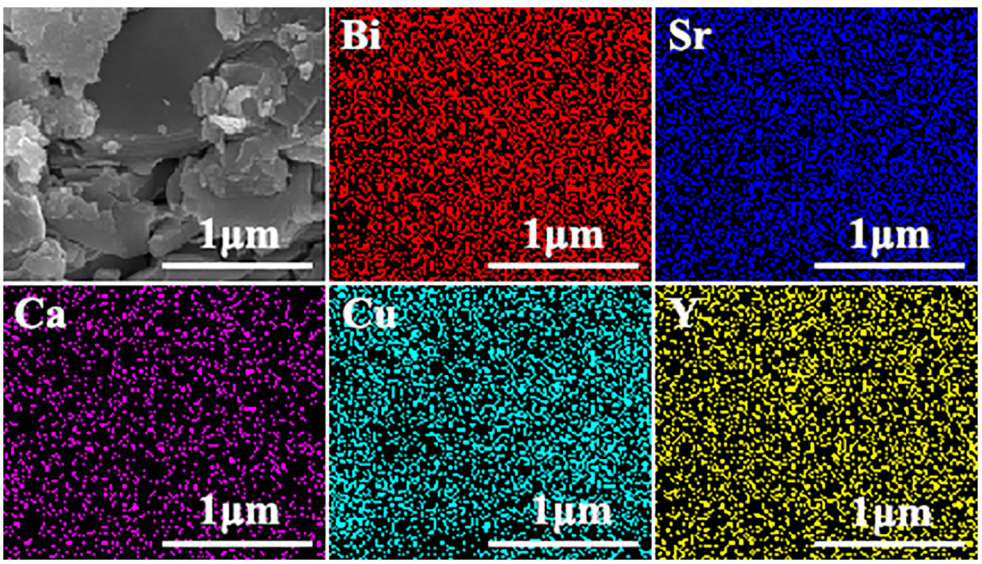

Fig. 5 SEM image and chemical element distribution map of B(P)SCCO doped with 0.5 wt% Y_2O_3:Eu^{3+}+Ag (A4)

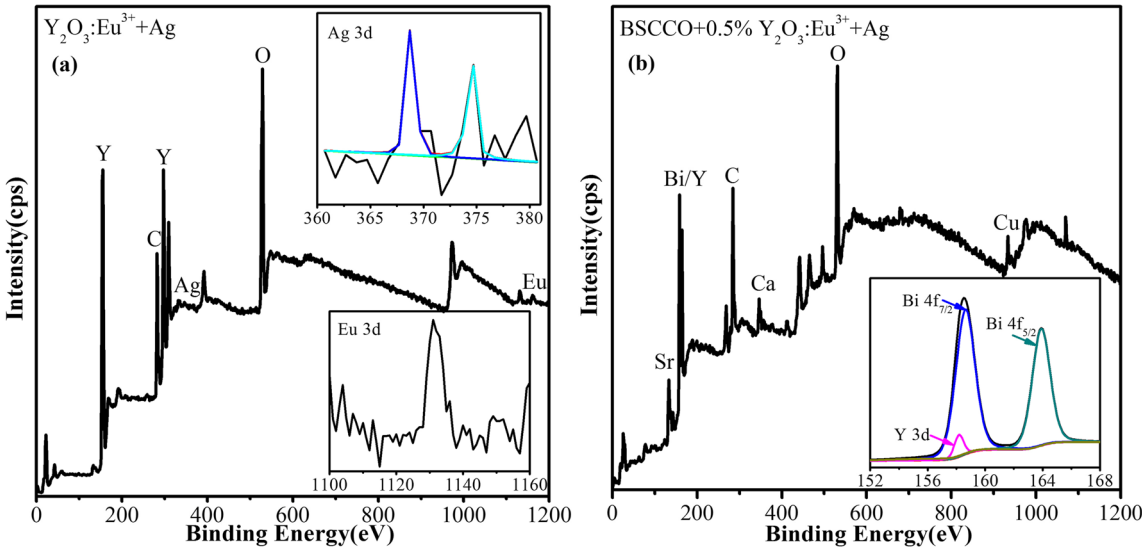

Fig. 6 **a** XPS spectra of Y_2O_3:Eu^{3+}+Ag, the insets show the magnified Ag 3d and Eu 3d spectra; **b** XPS spectra of B(P)SCCO doped with 0.5 wt% Y_2O_3:Eu^{3+}+Ag (A4), the inset shows the magnified Bi 4f and Y 3d spectra

topological luminophore are increased by 8 K and 4 K, respectively. However, the T_C of B(P)SCCO doped with 0.2 wt% Y_2O_3 and 0.2 wt% Y_2O_3:Sm^{3+} nonluminous inhomogeneous phases show a decrease. This finding confirms that the increase of transition temperature is the effect of EL rather than the influence of rare earth elements.

We found that the purity of raw materials and test status are the root causes of the poor quality of the samples and transition curves. So we changed the purity of raw materials from 99 to 99.99%, the quality of the sample improved, the volume fraction of Bi-2223 increased from 46.8 to 74.3%, and the volume fraction of Bi-2212 decreased from 53.2 to 25.7%. $T_{C,0}$ increased from 57 to 67 K, and $T_{C,on}$ increased from 101 to 109.2 K. Figure 8a–d depict the normalized R–T curve of the pure B(P)SCCO with a raw materials purity of 99.99% (B1), and B(P)SCCO doped with 0.2 wt% Y_2O_3:Eu^{3+}+Ag (B2), Y_2O_3:Eu^{3+} (B3), Y_2O_3 (B4), and Y_2O_3:Sm^{3+} (B5) at different test currents. $T_{C,0}$ and $T_{C,on}$ can be obtained by the temperature dependence of dρ/dT (as shown in Fig. 8 e and f, test current $I = 0.1$ mA). In Fig. 8 e and f, the determination standards of $T_{C,0}$ and $T_{C,on}$ are defined, the zero resistance temperature $T_{C,0}$ is the temperature at which the resistance just completely drops to zero during the cooling process, and the onset transition temperature $T_{C,on}$ is the intersection of the extrapolated line and the temperature, $T_{C,0}$ and $T_{C,on}$ are determined using this standard in this experiment. Figure 9 shows the $T_{C,0}$ and $T_{C,on}$ with error bars for B1, B2, B3, B4, and B5 at $I = 100$, 10, 1, and 0.1 mA. It can be seen that although $T_{C,0}$ and $T_{C,on}$ have a certain change, the change is small, indicating that prepared samples have better stability, and the experimental results are more reliable. The average value of transition temperatures are listed in Table 3. With the test current I decreases from 100 to 0.1 mA, $T_{C,0}$ of pure B(P)SCCO increases from 67 to 89 K, and $T_{C,on}$ remains unchanged ($T_{C,on} = 109.2$ K). When $I = 1$ mA and 0.1 mA, the transition temperature of pure B(P)SCCO is 80.5–109.2 and 89–109.2 K, respectively, and the transition width is small. At the same time, we found that doping of Y_2O_3 and

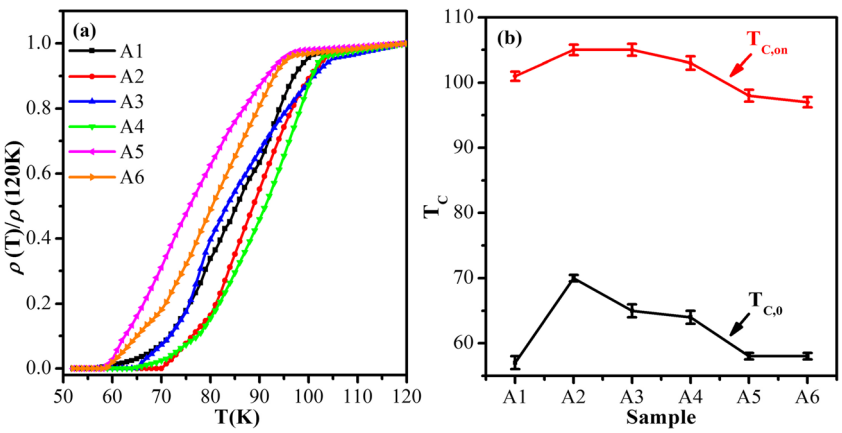

Fig. 7 **a** Temperature-dependent normalized resistivity curves of pure B(P)SCCO (A1) and B(P)SCCO doped with 0.1 wt% Y_2O_3:Eu^{3+}+Ag (A2), 0.2 wt% Y_2O_3:Eu^{3+}+Ag (A3), 0.5 wt% Y_2O_3:Eu^{3+}+Ag (A4), 0.2 wt% Y_2O_3 (A5), and 0.2 wt% Y_2O_3:Sm^{3+} (A6); **b** $T_{C,0}$ and $T_{C,on}$ of A1, A2, A3, A4, A5, and A6

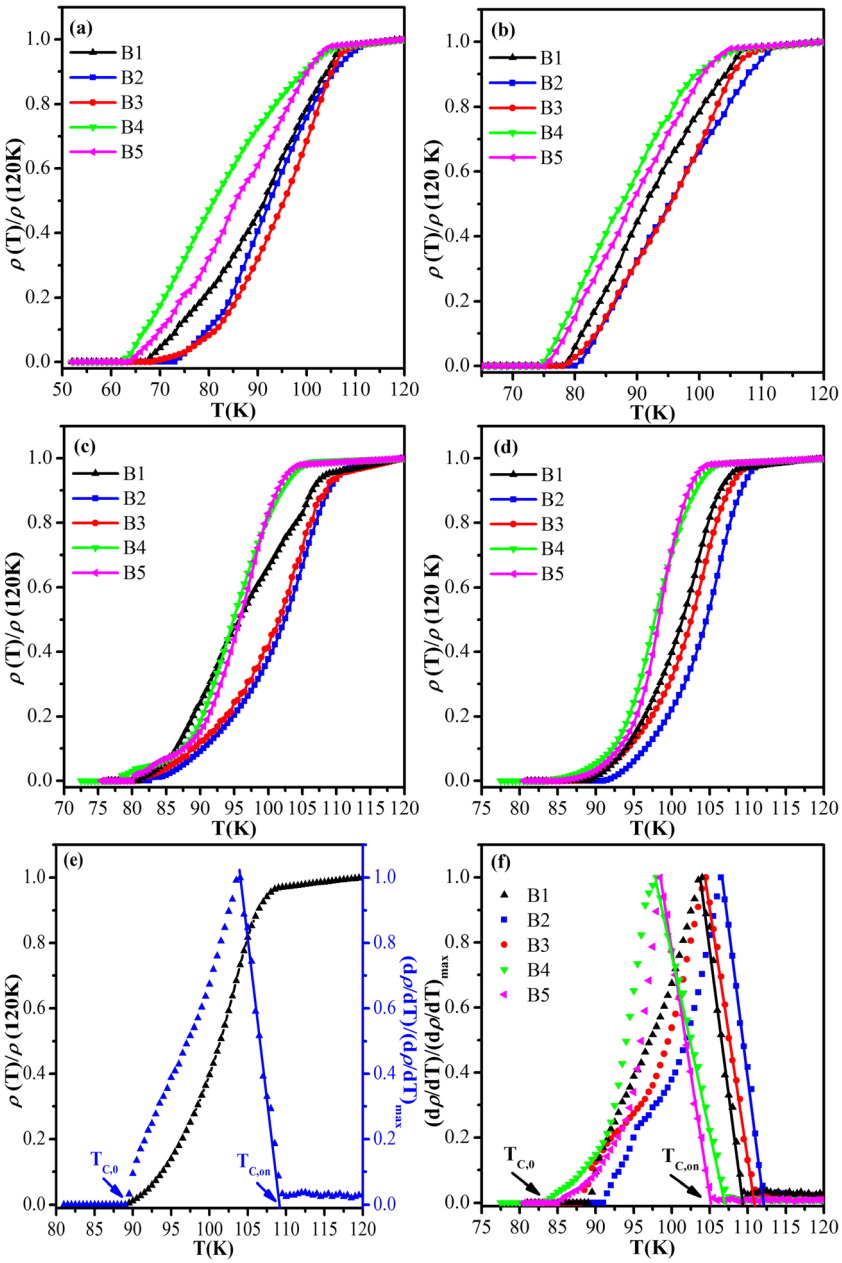

Fig. 8 Temperature-dependent normalized resistivity curves of pure B(P)SCCO (B1) and B(P)SCCO doped with 0.2 wt% Y_2O_3:Eu^{3+}+Ag (B2), 0.2 wt% Y_2O_3:Eu^{3+} (B3), 0.2 wt% Y_2O_3 (B4), and 0.2 wt% Y_2O_3:Sm^{3+} (B5) at **a** 100 mA, **b** 10 mA, **c** 1 mA, and **d** 0.1 mA; Temperature dependence of normalized dρ/dT of **e** B1, **f** B1, B2, B3, B4, and B5 at I = 0.1 mA

Y_2O_3:Sm^{3+} nonluminous dopants reduces the transition temperature of B(P)SCCO: however, Y_2O_3:Eu^{3+} and Y_2O_3:Eu^{3+}+Ag luminous inhomogeneous phases doping increases the transition temperature of B(P)SCCO by 2~3 K.

This experiment indicates that the T_C of B(P)SCCO increased by doping with Y_2O_3:Eu^{3+}+Ag or Y_2O_3:Eu^{3+} luminophore. However, Jiang et al. [36] found that the T_C of B(P)SCCO doped with 1 wt% ZnO EL material decreased compared with pure B(P)SCCO in 2007. Two experiments present different results, which may be explained by the following reasons: the microstructure of ZnO dopants are spherical or ellipsoid, whereas, the Y_2O_3:Eu^{3+}+Ag or Y_2O_3:Eu^{3+} luminophore used in this experiment exhibits a flake structure, this structure can further improve the dispersion and connectivity, thereby, making the dispersion more uniform, better connectivity, and more consistent with the proposed model. And ZnO EL intensity is extremely weak, the EL intensity of Y_2O_3:Eu^{3+}+Ag or Y_2O_3:Eu^{3+} luminophore in this experiment is considerably stronger than that of ZnO. Meanwhile, the doping concentration of ZnO is extremely high.

The superconducting mechanism of the traditional MgB_2 superconductor is the interaction of electron and phonon, and the transformation of electrons into cooper pairs can be enhanced via EL energy injection by doping with Y_2O_3:Eu^{3+} EL materials in MgB_2 superconductor, thereby, enhancing T_C of MgB_2 [45–47]. In this experiment, the $T_{C,0}$ and $T_{C,on}$ of high-temperature superconductor B(P)SCCO increased by doping

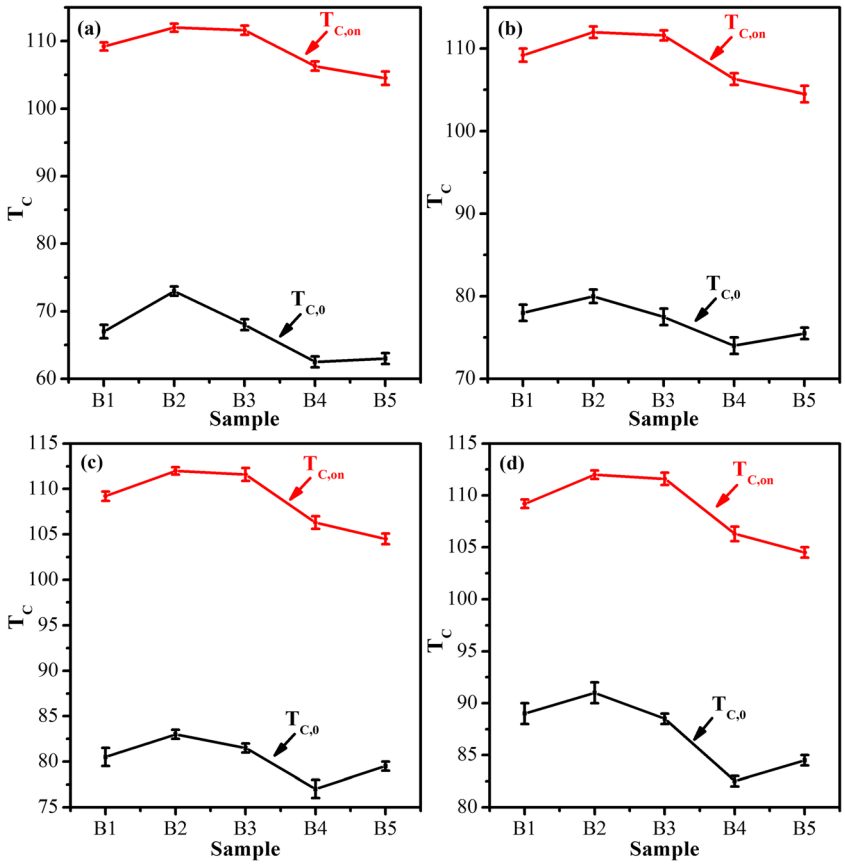

Fig. 9 $T_{C,0}$ and $T_{C,on}$ of B1, B2, B3, B4, and B5 at **a** 100 mA, **b** 10 mA, **c** 1 mA, and **d** 0.1 mA

with Y_2O_3:Eu^{3+}+Ag or Y_2O_3:Eu^{3+} luminophore, which may be due to electron pairs are formed on the basis of the magnetic interaction of electron spin in the high-temperature B(P)SCCO superconductor, and the EL energy injection of Y_2O_3:Eu^{3+}+Ag or Y_2O_3:Eu^{3+} luminophore promotes the formation of electron pairs, thus the T_C of B(P)SCCO increased. Of course, this increase may also be related to the creation of charge carriers by doping the conduction bands [54–57]. The mechanism for enhancing the T_C is unclear and requires further exploration.

In this experiment, the relative variation of T_C of luminous inhomogeneous phase doping is different when the sample quality is different. Whether further improvement of composition will reduce the effect of the luminophore doping on T_C also requires further exploration in subsequent experiments.

5 Conclusion

Based on the idea that injecting energy will promote the formation of electron pairs, a smart meta-superconductor B(P)SCCO is constructed according to the method of metastructure, which consists of B(P)SCCO particles and Y_2O_3:Eu^{3+}+Ag or Y_2O_3:Eu^{3+} luminophore to form a composite particle structure. In the local electric field, the B(P)SCCO

Table 3 Summary of the volume content and critical temperature of B1, B2, B3, B4 and B5

Sample	Bi-2223 (%)	Bi-2212 (%)	$T_{C,0}$ (K); $T_{C,on}$ (K)			
			100 mA	10 mA	1 mA	0.1 mA
B1	74.3	25.7	67; 109.2	78; 109.2	80.5; 109.2	89; 109.2
B2	74.2	25.8	73; 112	80; 112	83; 112	91; 112
B3	74.5	25.5	68; 110.8	77.5; 110.8	81.5; 110.8	88.5; 110.8
B4	74.4	25.6	62.5; 106.8	74; 106.8	77; 106.8	82.5; 106.8
B5	74.7	25.3	63; 105.2	75.5; 105.2	80; 105.2	84.5; 105.2

superconducting particles act as microelectrodes, which stimulate the EL of Y_2O_3:Eu^{3+}+Ag or Y_2O_3:Eu^{3+} luminophore, thereby improving the T_C by EL energy injection.

A series of low-purity and high-purity B(P)SCCO samples doped with different dopants were experimentally prepared. The prepared samples are randomly oriented and exhibit an irregular blocky structure, and the addition of dopants does not affect the formation and microstructure of B(P)SCCO. We performed *R-T* tests on all prepared samples at the test current $I = 100$ mA, and find that Y_2O_3 or Y_2O_3:Sm^{3+} nonluminous inhomogeneous phase doping makes T_C lower than pure sample, while Y_2O_3:Eu^{3+} or Y_2O_3:Eu^{3+}+Ag luminous inhomogeneous phase doping makes T_C higher than pure sample.

When the test current I decreases from 100 to 0.1 mA, $T_{C,0}$ of high-purity samples increases, and $T_{C,on}$ remains unchanged. And when the test currents $I = 10$, 1, and 0.1 mA, we still find that the T_C of Y_2O_3 or Y_2O_3:Sm^{3+} nonluminous inhomogeneous phase–doped sample is lower than that of the pure sample, and the T_C of Y_2O_3:Eu^{3+} or Y_2O_3:Eu^{3+}+Ag luminous inhomogeneous phase doped sample is higher than that of the pure sample. This outcome may be that the Y_2O_3:Eu^{3+}+Ag or Y_2O_3:Eu^{3+} luminophore generates an EL under the action of an applied electric field, thereby improving the T_C of B(P)SCCO via energy injection.

It is significant to improve the T_C of high-temperature superconductor B(P)SCCO; in this study, we construct a smart meta-superconductor B(P)SCCO to promote the formation of electron pairs via EL energy injection; this provides a new idea for improving the T_C and practical application of high-temperature superconductors.

Funding information This work was supported by the National Natural Science Foundation of China for Distinguished Young Scholar under Grant No. 50025207.

References

1. Fausti, D., Tobey, R.I., Dean, N., Kaiser, S., Dienst, A., Hoffmann, M.C., Pyon, S., Takayama, T., Takagi, H., Cavalleri, A.: Light-induced superconductivity in a stripe-ordered cuprate. Science. **331**(6014), 189–191 (2011)
2. Dienst, A., Casandruc, E., Fausti, D., Zhang, L., Eckstein, M., Hoffmann, M., Khanna, V., Dean, N., Gensch, M., Winnerl, S., Seidel, W., Pyon, S., Takayama, T., Takagi, H., Cavalleri, A.: Optical excitation of Josephson plasma solitons in a cuprate superconductor. Nat. Mater. **12**(6), 535–541 (2013)
3. Hu, W., Kaiser, S., Nicoletti, D., Hunt, C.R., Gierz, I., Hoffmann, M.C., Le Tacon, M., Loew, T., Keimer, B., Cavalleri, A.: Optically enhanced coherent transport in $YBa_2Cu_3O_{6.5}$ by ultrafast redistribution of interlayer coupling. Nat. Mater. **13**(7), 705–711 (2014)
4. Mitrano, M., Cantaluppi, A., Nicoletti, D., Kaiser, S., Perucchi, A., Lupi, S., Di Pietro, P., Pontiroli, D., Ricco, M., Clark, S.R., Jaksch, D., Cavalleri, A.: Possible light-induced superconductivity in K_3C_{60} at high temperature. Nature. **530**(7591), 461–464 (2016)
5. Cantaluppi, A., Buzzi, M., Jotzu, G., Nicoletti, D., Mitrano, M., Pontiroli, D., Ricco, M., Perucchi, A., Di Pietro, P., Cavalleri, A.: Pressure tuning of light-induced superconductivity in K_3C_{60}. Nat. Phys. **14**(8), 837–841 (2018)
6. Maeda, H., Tanaka, Y., Fukutomi, M., Asano, T.: A new high-T_C oxide superconductor without a rare earth element. Jpn. J. Appl. Phys. **27**(2), L209–L210 (1988)
7. Tarascon, J.M., LePage, Y., Greene, L.H., Bagley, B.G., Barboux, P., Hwang, D.M., Hull, G.W., McKinnon, W.R., Giroud, M.: Origin of the 110-K superconducting transition in the Bi-Sr-Ca-Cu-O system. Phys. Rev. B. **38**(4), 2504–2508 (1988)
8. Tarascon, J.M., McKinnon, W.R., Barboux, P., Hwang, D.M., Bagley, B.G., Greene, L.H., Hull, G.W., LePage, Y., Stoffel, N., Giroud, M.: Preparation, structure, and properties of the superconducting compound series $Bi_2Sr_2Ca_{n-1}Cu_nO_y$ with n=1,2, and 3. Phys. Rev. B. **38**(13), 8885–8892 (1988)
9. Onellion, M., Tang, M., Chang, Y., Margaritondo, G., Tarascon, J.M., Morris, P.A., Bonner, W.A., Stoffel, N.G.: Photoemission study of the new high-temperature superconductor Bi-Ca-Sr-Cu-O. Phys. Rev. B. **38**(1), 881–884 (1988)
10. Gao, L., Huang, J.Z., Meng, L.R., Hor, H.P., Bechtold, J., Sun, Y.Y., Chu, W.C., Sheng, Z.Z., Herman, M.A.: Bulk superconductivity in $Tl_2CaBa_2Cu_2O_{8+\delta}$ up to 120 K. Nature. **332**, 623–624 (1988)
11. Hazen, R.M., Prewitt, C.T., Angel, R.J., Ross, N.L., Finger, L.W., Hadidiacos, C.G., Veblen, D.R., Heaney, P.J., Hor, P.H., Meng, R.L., Sun, Y.Y., Wang, Y.Q., Xue, Y.Y., Huang, Z.J., Gao, L., Bechtold, J., Chu, C.W.: Superconductivity in the high-T_C Bi-Ca-Sr-Cu-O system: phase identification. Phys. Rev. Lett. **60**(12), 1174–1177 (1988)
12. Tallon, L.J., Buckley, G.R., Gilbert, W.P., Presland, R.M., Brown, M.W.I., Bowder, E.M., Christian, A.L., Gafull, R.: High-T_C superconducting phases in the series $Bi_{2.1}(Ca, Sr)_{n+1}Cu_nO_{2n+4+\delta}$. Nature. **333**, 153–156 (1988)
13. Majewsky, P., Hettich, B., Schulze, K., Petzow, G.: Preparation of unleaded $Bi_2Sr_2Ca_2Cu_3O_{10}$. Adv. Mater. **3**, 488–491 (1991)
14. Michel, C., Hervieu, M., Borel, M.M., Grandin, A., Deslandes, F., Provost, J., Raveau, B.: Superconductivity in the Bi-Sr-Cu-O system. Z. Phy. B- Condensed Matter. **68**, 421–423 (1987)
15. Ikeda, Y., Takano, M., Hiroi, Z., Oda, K., Kitaguchi, H., Takada, J., Miura, Y., Takeda, Y., Yamamoto, O., Mazaki, H.: The high-T_C phase with a new modulation mode in the bi, Bi, Pb-Sr-Ca-Cu-O System. Jpn J Appl Phys. **27**(11), L2067–L2070 (1988)
16. Majewski, P.: BiSrCaCuO high-T_C superconductors. Adv. Mater. **6**(6), 460–469 (1994)
17. Majewski, P.: New HTSCs-still far below room temperature. Adv. Mater. **5**, 862–864 (1993)
18. Chen, Y.L., Stevens, R.: 2223 phase formation in Bi(Pb)-Sr-Ca-Cu-O: II, The Role of Temperature- Reaction Mechanism. J. Am. Ceram. Soc. **75**(5), 1150–1159 (1992)
19. Chen, Y.L., Stevens, R.: 2223 phase formation in Bi(Pb)-Sr-Ca-Cu-O: III, The Role of Atmosphere. J. Am. Ceram. Soc. **75**(5), 1160–1166 (1992)
20. Chen, Y.L., Stevens, R.: 2223 phase formation in Bi(Pb)-Sr-Ca-Cu-O: I, The Role of Chemical Composition. J. Am. Ceram. Soc. **75**(5), 1142–1149 (1992)
21. Mujewski, P., Kuesche, S., Aldinger, F.: Fundamentals of the preparation of high-T_C superconducting $(Bi,Pb)_{2+x}Sr_2Ca_2Cu_3O_{10+\delta}$ ceramics. Adv. Mater. **8**(9), 762–765 (1996)
22. Hudakova, N., Plechacek, V., Dordor, P., Flachbart, K., Knizek, K., Kovac, J., Reiffers, M.: Influence of Pb concentration on microstructural and superconducting properties of BSCCO superconductors. Supercond. Sci. Technol. **8**, 324–328 (1995)
23. Asghari, R., Naghshara, H., Arsalan, L.Ç., Sedghi, H.: Comparing the effects of Nb, Pb, Y, and La replacement on the structural, electrical, and magnetic characteristics of Bi-based superconductors. J. Supercond. Nov. Magn. **31**(12), 3889–3898 (2018)

24. Zhigadlo, N.D., Petrashko, V.V., Semenenko, Y.A., Panagopoulos, C., Cooper, J.R., Salje, E.K.H.: The effects of Cs doping, heat treatments on the phase formation and superconducting properties of (Bi,Pb)-Sr-Ca-Cu-O ceramics. Physica C Supercond. **299**(3–4), 327–337 (1998)
25. Chu, C.W., Bechtold, J., Gao, L., Hor, P.H., Huang, Z.J., Meng, R.L., Sun, Y.Y., Wang, Y.Q., Xue, Y.Y.: Superconductivity up to 114 K in the Bi-Al-Ca-Sr-Cu-O compound system without rare-earth elements. Phys. Rev. Lett. **60**(10), 941–943 (1988)
26. Özçelik, B., Kaya, C., Gündoğmuş, H., Sotelo, A., Madre, M.A.: Effect of Ce substitution on the Magnetoresistivity and flux pinning energy of the $Bi_2Sr_2Ca_{1-x}Ce_xCu_2O_{8+\delta}$ superconductors. J. Low Temp. Phys. **174**(3–4), 136–147 (2013)
27. Annabi, M., M'Chirgui, A., Ben Azzouz, F., Zouaoui, M., Ben Salem, M.: Addition of nanometer Al_2O_3 during the final processing of (Bi,Pb)-2223 superconductors. Physica C Supercond. **405**(1), 25–33 (2004)
28. Yavuz, Ş., Bilgili, Ö., Kocabaş, K.: Effects of superconducting parameters of SnO_2 nanoparticles addition on (Bi,Pb)-2223 phase. J. Mater. Sci. Mater. Electron. **27**(5), 4526–4533 (2016)
29. Jia, Z.Y., Tang, H., Yang, Z.Q., Xing, Y.T., Wang, Y.Z., Qiao, G.W.: Effects of nano-ZrO_2 particles on the superconductivity of Pb-doped BSCCO. Physica C Supercond. **337**, 130–132 (2000)
30. Guilmeau, E., Andrzejewski, B., Noudem, J.G.: The effect of MgO addition on the formation and the superconducting properties of the Bi2223 phase. Physica C Supercond. **387**(3–4), 382–390 (2003)
31. Abbasi, H., Taghipour, J., Sedghi, H.: The effect of $MgCO_3$ addition on the superconducting properties of Bi2223 superconductors. J. Alloys Compd. **482**, 552–555 (2009)
32. Eremina, E.A., Kravchenko, A.V., Kazin, P.E., Tretyakov, Y.D., Jansen, M.: Influence of boron-containing dopants on the formation of superconducting phase in the system Bi(Pb)-Sr-Ca-Cu-O. Supercond. Sci. Technol. **11**(2), 223–226 (1998)
33. Xu, S.H., Zhou, Y.W., Zhao, X.P.: Research and Development of inorganic powder EL materials. Materials Review. **21**(11), 162–166 (2007) in Chinese, available at http://www.cnki.com.cn/Article/CJFDTotal-CLDB2007S3048.htm. Accessed 28 Apr 2020.
34. Liu, H., Zhao, X.P., Yang, Y., Li, Q.W., Lv, J.: Fabrication of infrared left-handed Metamaterials via double template-assisted electrochemical deposition. Adv. Mater. **20**(11), 2050–2054 (2008)
35. Zhao, X.P.: Bottom-up fabrication methods of optical metamaterials. J. Mater. Chem. **22**(19), 9439–9449 (2012)
36. Jiang, W.T., Xu, Z.L., Chen, Z., Zhao, X.P.: Introduce uniformly distributed ZnO nano-defects into BSCCO superconductors by nano-composite method. J. Funct. Mater. **38**(01), 157–160 (2007) in Chinese, available at http://www.cnki.com.cn/Article/CJFDTOTAL-GNCL200701046.htm. Accessed 28 Apr 2020.
37. Wang, M.Z., Xu, L.X., Chen, G.W., Zhao, X.P.: Topological luminophor Y_2O_3:Eu^{3+}+Ag with high electroluminescence performance. ACS Appl. Mater. Interfaces. **11**(2), 2328–2335 (2019)
38. Patra, A., Friend, C.S., Kapoor, R., Prasad, P.N.: Upconversion in Er^{3+}:ZrO_2 Nanocrystals. J. Phys. Chem. B. **106**(8), 1909–1912 (2002)
39. Zhang, Y.X., Guo, J., White, T., Tan, T.T.Y., Xu, R.: Y_2O_3:Tb Nanocrystals self-assembly into Nanorods by oriented attachment mechanism. J. Phys. Chem. C. **111**(22), 7893–7897 (2007)
40. Smolyaninov, I.I., Smolyaninova, V.N.: Is there a Metamaterial route to high temperature superconductivity? Adv. Cond. Matter Phys. **2014**, 479635 (2014)
41. Smolyaninova, V.N., Yost, B., Zander, K., Osofsky, M.S., Kim, H., Saha, S., Greene, R.L.: Smolyaninov, II: experimental demonstration of superconducting critical temperature increase in electromagnetic metamaterials. Sci. Rep. **4**, 7321 (2014)
42. Smolyaninov, I.I., Smolyaninova, V.N.: Theoretical modeling of critical temperature increase in metamaterial superconductors. Phys. Rev. B. **93**, 184510 (2016)
43. Zhang, Z.W., Tao, S., Chen, G.W., Zhao, X.P.: Improving the critical temperature of MgB_2 superconducting Metamaterials induced by electroluminescence. J. Supercond. Nov. Magn. **29**(5), 1159–1162 (2016)
44. Tao, S., Li, Y.B., Chen, G.W., Zhao, X.P.: Critical temperature of smart meta-superconducting MgB_2. J. Supercond. Nov. Magn. **30**(6), 1405–1411 (2017)
45. Li, Y.B., Chen, H.G., Qi, W.C., Chen, G.W., Zhao, X.P.: Inhomogeneous phase effect of smart meta-superconducting MgB_2. J. Low Temp. Phys. **191**, 217–227 (2018)
46. Chen, H.G., Li, Y.B., Chen, G.W., Xu, L.X., Zhao, X.P.: The effect of inhomogeneous phase on the critical temperature of smart meta-superconductor MgB_2. J. Supercond. Nov. Magn. **31**(10), 3175–3182 (2018)
47. Li, Y.B., Chen, H.G., Wang, M.Z., Xu, L.X., Zhao, X.P.: Smart meta-superconductor MgB_2 constructed by inhomogeneous phase of luminescent nanocomposite. Sci. Rep. **9**(1), 14194 (2019)
48. Damascelli, A., Hussain, Z., Shen, Z.X.: Angle-resolved photoemission studies of the cuprate superconductors. Rev. Mod. Phys. **75**, 473–541 (2003)
49. Bok, J.M., Bae, J.J., Choi, H.-Y., Varma, C.M., Zhang, W.T., He, J.F., Zhang, Y.X., Yu, L., Zhou, X.J.: Quantitative determination of pairing interactions for high-temperature superconductivity in cuprates. Sci. Adv. **2**(3), e1501329 (2016)
50. Zhao, X.P., Chen, H.G., Li, Y.B., Wang, M.Z.: Meta-superconductor Bi(Pb)-Sr-Ca-Cu-O constructeded by topological luminophor inhomogeneous phase and its preparation method. Chinese Patent 201910184673.X
51. Driessche, I.V., Buekenhoudtt, A., Konstantinov, K., Bruneel, E., Hoste, S.: Evaluation of the phase composition of BPSCCO bulk samples by XRD- and susceptibility analysis. Appl. Supercond. **4**(4), 185–190 (1996)
52. Mukherjee, P.S., Simon, A., Koshy, J., Guruswamy, P., Damodaran, A.D.: Superconductivity in Ag added Bi-Sr-Ca-Cu-O system. Solid State Commun. **76**(5), 659–661 (1990)
53. Terzioglu, C., Yilmazlar, M., Ozturk, O., Yanmaz, E.: Structural and physical properties of Sm-doped $Bi_{1.6}Pb_{0.4}Sr_2Ca_{2-x}Sm_xCu_3O_y$ superconductors. Physica C Supercond. **423**(3–4), 119–126 (2005)
54. Yu, G., Lee, C.H., Heeger, A.J.: Photo-excitation of single crystals of $La_2CuO_{4+\delta}$ near the metal-insulator transition. Physica C Supercond. **190**, 563–568 (1992)
55. Kudinov, V.I., Chaplygin, I.L., Kirilyuk, A.I., Kreines, N.M., Laiho, R., Lahderanta, E., Ayache, C.: Persistent photoconductivity in $YBa_2Cu_3O_{6+x}$ films as a method of photodoping toward metallic and superconducting phases. Phys. Rev. B. **47**(14), 9017–9028 (1993)
56. Sinha, K.P.: Photon-induced superconducting phase transition in some cuprates. Physica C Supercond. **212**, 128–132 (1993)
57. Yu, G., Heeger, A.J.: Photoinduced charge carriers in insulating cuprates fermi glass insulator, metal-insulator transition and superconductivity. Int J Mod Phys B. **7**(22), 3751–3815 (1993)